27

Traditional and Dynamic Action Potential Clamp Experiments with HCN4 Pacemaker Current: Biomedical Engineering in Cardiac Cellular Electrophysiology

Arie O. Verkerk and Ronald Wilders
Heart Failure Research Center, Academic Medical Center, University of Amsterdam
The Netherlands

1. Introduction

The sinoatrial (SA) node is the normal pacemaker of the mammalian heart and generates the electrical impulse for the regular, rhythmic contraction of the heart. Pacemaker activity—or spontaneous electrical activity—of SA nodal cells is based on the presence of a special phase of the action potential, the diastolic depolarization, in which cells depolarize spontaneously towards the action potential threshold. This diastolic depolarization phase is due to a very small net inward current across the cell membrane, which is the result of a complex interaction of multiple inwardly and outwardly directed ion currents (see reviews by Boyett et al. (2000), Dobrzynski et al. (2007), and Mangoni & Nargeot (2008)). Among these currents, the hyperpolarization-activated 'funny' current (I_f) is of particular importance and is traditionally also named 'pacemaker current'. The ion channels carrying I_f are encoded by the hyperpolarization-activated cyclic nucleotide-modulated (HCN) gene family, with HCN4 as the dominant HCN isoform in the SA node (Moosmang et al., 2001; Dobrzynski et al., 2007). Despite a large body of experimental data from voltage clamp experiments, the contribution of I_f to pacemaker activity in the adult SAN is still controversial and not fully established (see Verkerk et al. (2009a) and primary references cited therein).

In this chapter, we demonstrate how the 'action potential clamp' technique, as an alternative to traditional voltage clamp, can provide insights into the role of I_f in SA nodal pacemaker activity. We have used the action potential clamp technique to study the behaviour of HCN4 channels expressed—by transfection with the ion channel gene cDNA—in cells from the HEK-293 human embryonic kidney cell line, which express little or no endogenous HCN channels (Varghese et al., 2006). The current in response to a voltage clamp command potential with the shape of an SA nodal action potential then reflects the behaviour of the expressed HCN4 channels during that action potential. We also show how this technique can be turned into a dynamic technique with continuous feedback between the SA nodal action potential and the HEK-293 cell current. With this 'dynamic action potential clamp' technique, the voltage clamp command potential is not a predefined action potential, but is the free-running membrane potential of an SA nodal cell that is simulated in real time, with

the measured HEK-293 cell current contributing to its net membrane current. In this approach, it is immediately clear how the HCN4 channels affect the SA nodal action potential.

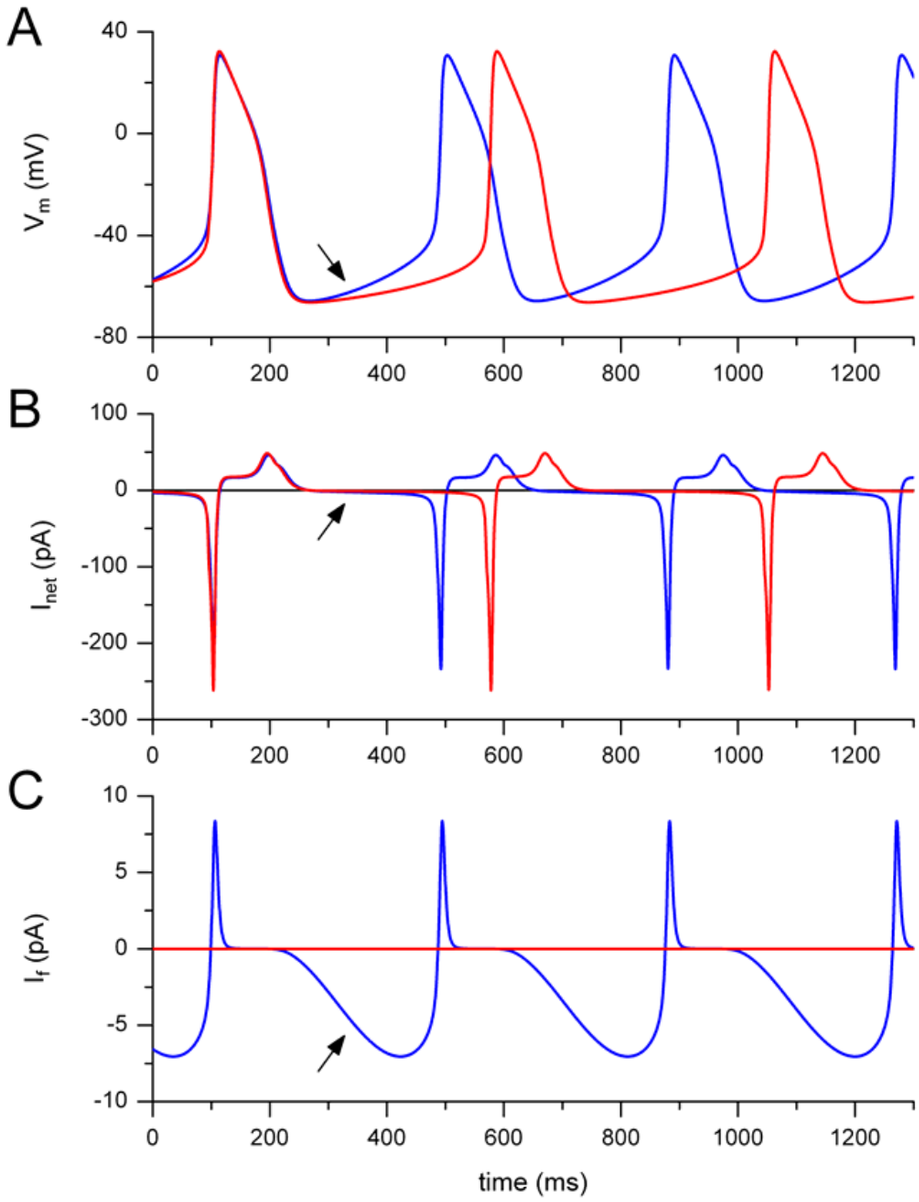

Fig. 1. Pacemaker activity a single pacemaker cell isolated from the rabbit sinoatrial node. Computer simulation using the Wilders et al. (1991) model under control conditions (blue traces) and with the hyperpolarization-activated 'pacemaker current' I_f set to zero (red traces). (A) Spontaneous action potentials. (B) Underlying net membrane current (I_{net}). (C) Hyperpolarization-activated current (I_f). Note difference in ordinate scales between panels B and C.

2. Pacemaker activity of the sinoatrial node

Figure 1 illustrates the intrinsic pacemaker activity of the cells that constitute the SA node. Figure 1A (blue trace) shows spontaneous action potentials of a rabbit SA nodal cell, according to the mathematical model of such cell by Wilders et al. (1991). The arrow indicates the diastolic depolarization phase of the action potential, during which the cell undergoes a spontaneous depolarization towards the action potential threshold. Figure 1B (blue trace) shows the net current across the cell membrane (I_{net}) that charges and discharges the membrane capacitance and underlies the spontaneous electrical activity. By convention, a net inward inflow of cations, which depolarizes the cell, is shown as a negative current. During diastolic depolarization, I_{net} is a tiny net inward current (arrow), which results from a complex interaction of several inwardly and outwardly directed cation currents. On a different ordinate scale, Figure 1C (blue trace) shows the 'pacemaker current' I_f, which makes an important contribution to this net inward current (arrow). Note that I_f turns into an outward current during the subsequent upstroke of the action potential, reflecting the I_f reversal potential of −24 mV. Although I_f is an important current, it is not a prerequisite for pacemaker activity. This is illustrated by the red traces in Fig. 1, which were obtained with the same action potential model, but with I_f set to zero. The main effect of 'blocking' I_f is a significant slowing of diastolic depolarization and an increase in the cycle length of the spontaneous electrical activity from 388 tot 474 ms (Fig. 1A).

3. Patch clamp

3.1 Recording from single cells

In today's cardiac cellular electrophysiology, 'patch clamp' is the common technique to

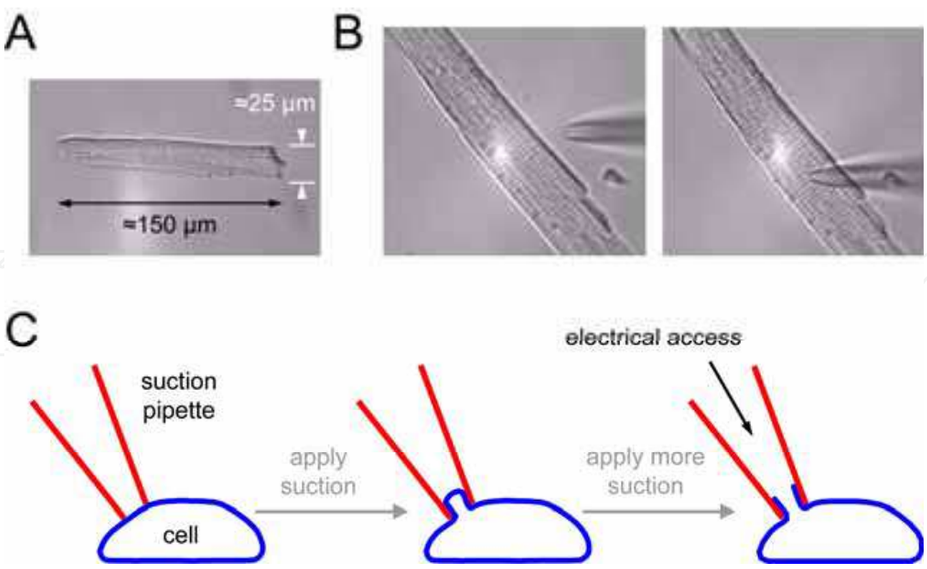

Fig. 2. Recording electrical activity of single cardiac myocytes. (A) Enzymatically isolated single ventricular myocyte. (B) Approaching the myocyte with a recording pipette. (C) Applying suction to obtain electrical access to the cell interior.

record the electrical activity of single cardiac cells, e.g. SA nodal cells. Cardiac myocytes are isolated from (pieces of) the hearts of laboratory animals by dedicated enzymatic isolation techniques. Cell suspensions are then put into a recording chamber on the stage of an inverted microscope and continuously superfused with Tyrode's solution, i.e. a salt solution with a composition in accordance with the interstitial fluid of the intact heart. Apparently healthy spindle or elongated spindle-like SA nodal cells or rod-shaped working myocardial cells with clear cross-striations (Fig. 2A) are selected for electrophysiological measurements. If not stimulated, pacemaker cells isolated from SA nodal tissue show regular rhythmic contractions, whereas cells isolated from atrial or ventricular tissue are quiescent.
For electrophysiological recording, pipettes are pulled from small borosilicate glass capillaries and heat polished. A pipette is filled with a salt solution mimicking the intracellular fluid. When filled with this 'pipette solution', the pipette typically has a 2–3 MΩ resistance, contributing to an unwanted 'series resistance', which can be electronically compensated by the 'patch clamp amplifier'. With the use of a micromanipulator that holds the pipette, the myocyte is approached with the recording pipette (Fig. 2B). When the pipette tip is in close vicinity of the myocyte (Fig. 2C, left), a little suction is applied and an omega-shaped seal is obtained (Fig. 2C, middle). If some more suction is applied, the seal is broken and electrical access to the cell interior is obtained (Fig. 2C, right). The thus obtained recording configuration is known as the 'whole-cell patch clamp configuration'.

3.2 Current clamp and voltage clamp

The 'whole-cell patch clamp configuration' of Fig. 2C (right) can be used in different recording modes. The main recording modes are 'current clamp' (Fig. 3A) and 'voltage clamp' (Fig. 3B). In either case, the bath solution is grounded to earth, as indicated by '$V = 0$' in Fig. 3A. In current clamp mode, the free-running membrane potential of the myocyte (V_m) is recorded. When recording from SA nodal myocytes, spontaneous action potentials, as in Fig. 1A, can be acquired. When recording from intrinsically quiescent cells, like atrial or ventricular myocytes, a brief current pulse can be injected into the myocyte through the

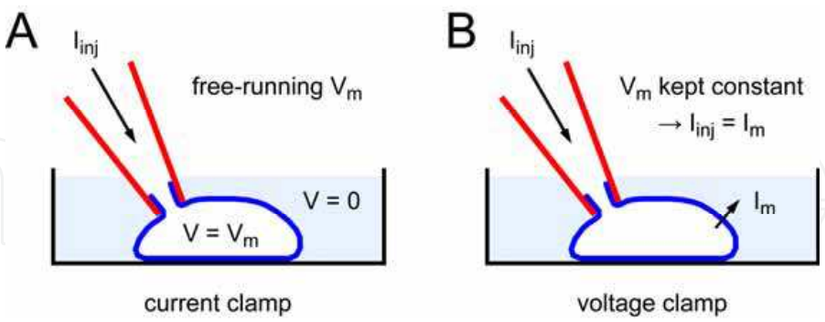

Fig. 3. Different recording modes of the whole-cell patch clamp configuration. (A) Current clamp mode. A current (I_{inj}) can be injected into the myocyte through the recording pipette, e.g. as a stimulus to elicit an action potential in a normally quiescent cell, and the free-running membrane potential of the myocyte (V_m) is recorded. (B) Voltage clamp mode. The membrane potential of the myocyte is held at a set level through a feedback circuit in the patch clamp amplifier. Consequently, the current that enters the cell through the recording pipette (I_{inj}) matches the current that leaves the cell through its membrane (I_m).

recording pipette as a stimulus to elicit an action potential (I_{inj}). In the voltage clamp mode, the membrane potential of the myocyte is held at a set level through a feedback circuit in the patch clamp amplifier. Consequently, there is no (dis)charging of the cell membrane capacitance and the current that enters the cell through the recording pipette (I_{inj}) matches the current that leaves the cell through its membrane (I_m). This way, ion currents can be studied under carefully controlled conditions, applying dedicated 'voltage clamp protocols' (cf. Section 4).

4. Voltage clamp recordings of HCN4 current

Figure 4 shows data obtained from voltage clamp experiments carried out on HEK-293 cells expressing HCN4 channels. The HCN4 gene was bicistronically expressed with green fluorescent protein (GFP) as a reporter of successful transfection with HCN4. Cell suspensions were put into a recording chamber on the stage of an inverted microscope, and superfused with Tyrode's solution (36±0.2°C) containing (in mmol/L): NaCl 140, KCl 5.4, $CaCl_2$ 1.8, $MgCl_2$ 1.0, glucose 5.5, and HEPES 5.0; pH was set to 7.4 with NaOH. Single HEK-293 cells exhibiting green fluorescence, indicating presence of HCN4 channels, were selected for electrophysiological measurements. The HCN4 current was recorded by the whole-cell patch clamp technique using an Axopatch 200B amplifier (Molecular Devices, Sunnyvale, CA, USA). The recording pipette was filled with a solution containing (in mmol/L): K-gluconate 125, KCl 20, NaCl 10, and HEPES 10; pH was set to 7.2 using KOH. Signals were low-pass filtered (cut-off frequency: 5 kHz) and digitized at 5 kHz. Series resistance was compensated by ≥80%, and potentials were corrected for the estimated 15 mV 'liquid junction potential'. Voltage control, data acquisition, and data analysis were accomplished using custom software.

Figure 4A shows representative HCN4 current recordings. The HCN4 current was measured during 6-s hyperpolarizing steps (range −30 to −120 mV) from a holding potential of −30 mV. Next, a 6-s step to −120 mV was applied to record 'tail current' followed by a 1-s pulse to 10 mV to ensure full deactivation (see Fig. 4A, top, for protocol; cycle length of protocol: 18 s). We observed large, time-dependent inward currents in response to the hyperpolarizing voltage steps (Fig. 4A, bottom). Typical for HCN4, the current amplitude and activation rate increased with more hyperpolarized potentials. The activation properties of the HCN4 current were measured during the 6-s hyperpolarizing steps. The average current voltage (I-V) relationship of the fully-activated HCN4 current at the end of the 6-s hyperpolarizing steps is shown in Fig. 4B. To correct for differences in current amplitude due to differences in cell size—larger cells have more channels in their membrane—currents were normalized to the cell membrane capacitance (in pF), which is a reliable measure of the cell membrane surface area.

The amplitude of the tail current immediately following the 6-s hyperpolarizing step reflects the amount of channels that activated during the preceding hyperpolarizing step. To characterize the voltage dependence of activation of the HCN4 current, we therefore plotted the normalized tail current amplitude (I/I_{max}) against the preceding hyperpolarizing potential. Average data are shown in Fig. 4C. The solid line is a Boltzmann fit to the data, for which we used the equation

$$I/I_{max} = A/\{\,1.0 + \exp[(V_m - V_{1/2})/k]\,\} \quad (1)$$

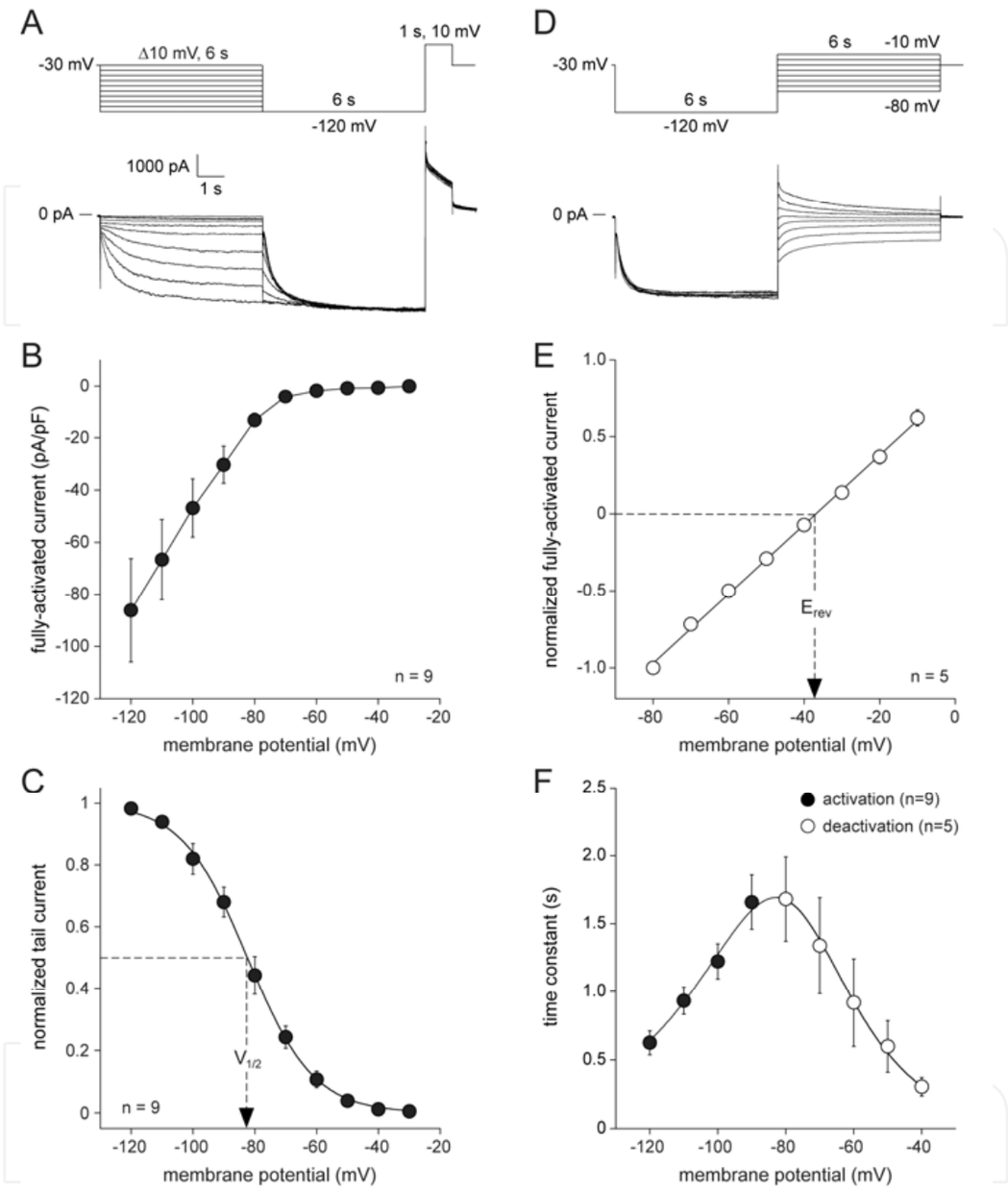

Fig. 4. Voltage clamp recordings of HCN4 current expressed in human embryonic kidney cells (HEK-293 cells). (A) Voltage pulse protocol to measure activation properties (top) and typical HCN4 current traces in response to this protocol (bottom). (B) Average current-voltage (I-V) relationship of the fully-activated HCN4 current at the end of the hyper-polarizing steps. (C) Voltage dependence of HCN4 current activation. Solid line is the Boltzmann fit to the experimental data. (D) Voltage pulse protocol to measure deactivation properties (top) and typical HCN4 current traces in response to this protocol (bottom). (E) I-V relationship of the fully-activated HCN4 current at the beginning of the depolarizing steps. Solid line is the linear fit to the experimental data. (F) Time constant of (de)activation.

In this equation, V_m denotes membrane potential and the fitting parameters $V_{1/2}$ and k are half-maximum activation voltage and slope factor, respectively. For the data of Fig. 4C, $V_{1/2}$ and k amounted to −87.7 ± 2.4 and 11.5 ± 2.4 mV (n=9), respectively.

Deactivation kinetics and reversal potential (E_{rev}) were measured during depolarizing steps (range −80 to −10 mV, duration 6 s) after a 6-s prepulse to −120 mV to ensure full activation (see Fig. 4D, top, for protocol and Fig. 4D, bottom, for a typical example of associated current recordings; cycle length of protocol: 15 s). E-4031 (5 μM) was added to the Tyrode's solution to block the delayed rectifier like endogenous current of HEK-293 cells (Yu & Kerchner, 1998; Jiang et al., 2002). The voltage dependence of the fully−activated current was evaluated over the entire range of depolarizing test potentials, i.e. −80 to −10 mV, by measuring the amplitude of the tail currents immediately following the 6-s hyperpolarizing step to −120 mV. Figure 4E shows the thus obtained average I-V relationship of the fully-activated HCN4 current normalized to its value measured at −120 mV. The average reversal potential was −36.8 ± 1.0 mV (n=5).

Activation of the HCN4 current during the hyperpolarizing steps of Fig. 4A was characterized by a monoexponential fit to each of the normalized current traces, using the equation

$$I/I_{max} = A \times [\, 1 - \exp(-t/\tau) \,] \quad (2)$$

In this equation, t denotes time and the fitting parameter τ is the time constant of activation. Similarly, deactivation of the HCN4 current during the depolarizing steps of Fig. 4D was characterized by a monoexponential fit to each of the normalized current traces, using the equation

$$I/I_{max} = A \times \exp(-t/\tau) \quad (3)$$

In this equation, t again denotes time and the fitting parameter τ now is the time constant of deactivation. In the above Eqs. 2 and 3, the variable initial delay in HCN4 current (de)activation is ignored (van Ginneken & Giles, 1991; Verkerk et al., 2009a). Figure 4F shows the average activation and deactivation time constants of the HCN4 current. The activation time constant (closed symbols) ranged from ≈625 ms at −120 mV to ≈1.6 s at −90 mV, and the deactivation time constant (open symbols) from ≈1.7 s at −80 mV to ≈305 ms at −40 mV. The bell-shaped curve in Fig. 4F was obtained by fitting the data to the equation

$$\tau = 1 \,/\, [\, A_1 \times \exp(-V_m/B_1) + A_2 \times \exp(V_m/B_2) \,] \quad (4)$$

In this equation, τ is the activation or deactivation time constant, V_m is membrane potential, and A_1, A_2, B_1, and B_2 are fitting parameters (Qu et al., 2004).

5. Action potential clamp

In this section, we first explain the traditional 'action potential clamp' technique and then the 'dynamic action potential clamp'. The techniques are presented by means of examples of recent applications aimed at investigating differences in kinetics of wild-type (WT) and mutant ion channels encoded by the human ether-à-go-go-related gene (HERG), i.e. the gene encoding the pore-forming α-subunit of the channels underlying the cardiac rapid delayed rectifier current (I_{Kr}). This outward potassium current is one of the ion currents underlying the repolarization phase of the action potential of ventricular cells (and also of SA nodal pacemaker cells).

5.1 Traditional action potential clamp

Essentially, action potential clamp is a particular refinement of the voltage clamp technique. Instead of the traditional step protocols (cf. Fig. 4, A and D), a prerecorded action potential waveform is used as voltage clamp command potential. Figure 5 shows a recent application

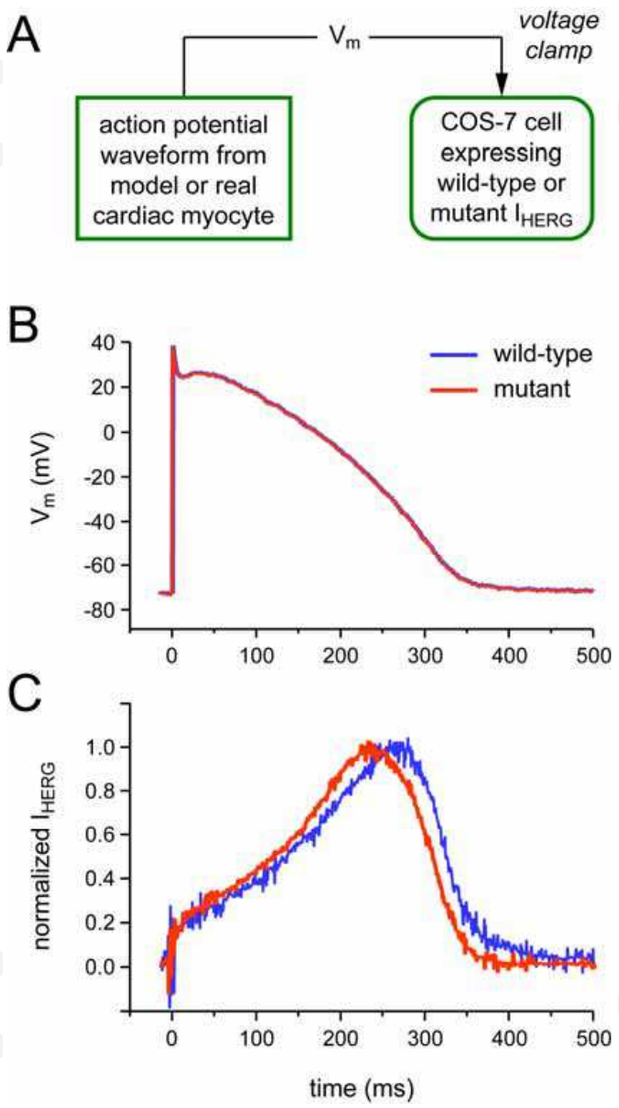

Fig. 5. Traditional action potential clamp experiment, exploring the effect of the A561P mutation in HERG. African green monkey kidney cells (COS-7 cells) were either transfected with human wild-type (WT) HERG cDNA or co-transfected with WT and A561P mutant HERG cDNA. (A) Experimental configuration. (B) Action potential recorded from a human ventricular myocyte, paced at 1 Hz, used as command voltage to clamp HERG-transfected COS-7 cells. Note that this command voltage is identical for WT ('wild-type', blue trace) and WT + A561P mutant ('mutant', red trace). (C) Normalized HERG current in response to the command voltage of B. Data from Bellocq et al. (2004).

of traditional action potential clamp by Bellocq et al. (2004) to investigate differences in kinetics of wild-type (WT) and A561P mutant HERG current. To this end, both WT + A561P mutant HERG channels, representing heterozygous carriers of the long-QT syndrome associated A561P mutation, and WT HERG channels, representing non-carriers, are expressed in the COS-7 cell line. Like HEK-293 cells, cells of this African green monkey cell line express little or no endogenous membrane current. As diagrammed in Fig. 5A, a previously recorded human ventricular action potential (Fig. 5B) is used as voltage clamp command potential and applied to HERG channel expressing COS-7 cells at a rate of 1 Hz. The associated normalized HERG current is shown in Fig. 5C. The current traces demonstrate a more rapid activation of WT + A561P current (red trace) compared to WT (blue trace), which would decrease action potential duration, but also a more rapid deactivation, which would increase action potential duration. From these data, it is difficult to predict the net effect of these changes in kinetics on the action potential. This is where dynamic action potential clamp can provide a direct and unambiguous answer.

5.2 Dynamic action potential clamp

'Dynamic clamp', which is widely used in neurophysiology but has its roots in cardiac electrophysiology (Wilders, 2005), has been used to introduce artificial conductances into real excitable cells by injecting a real-time computed current into a current-clamped cell, thus simulating, e.g., synaptic input in an isolated neuron or the presence of an additional membrane ionic current in an isolated cardiac cell (see reviews by Goaillard and Marder (2006) and Wilders (2006)). As a novel application of 'dynamic clamp', we recently developed the 'dynamic action potential clamp' (dAPC) technique, which was used to study the effects of ion channel mutations by effectively replacing a native ionic current of a cardiac myocyte with wild-type or mutant current expressed in HEK-293 cells (Berecki et al., 2005; Berecki et al., 2006; Berecki & van Ginneken, 2006; Berecki et al., 2007). Dynamic action potential clamp differs from traditional 'dynamic clamp' and 'action potential clamp' in that it combines current clamp, as used in dynamic clamp, and voltage clamp, as used in action potential clamp.

The diagram of Fig. 6A illustrates the concept of dynamic action potential clamp. Like in the study of Fig. 5, WT or mutant HERG channels are expressed in cells of a mammalian cell line, in this case HEK-293 instead of COS-7 cells, and subjected to voltage clamp to investigate differences in kinetic properties of these channels. This time, however, the voltage clamp command potential is not a prerecorded action potential, but the free-running membrane potential of a freshly isolated, patch-clamped ventricular cell (or cell model) with its native HERG-encoded current, i.e. I_{Kr}, blocked by a pharmacological agent (or set to zero in case of a model cell). The measured HERG current is injected into the ventricular myocyte in real time. Thus, there is continuous feedback between action potential and HERG current. The WT or mutant HERG channels are allowed to follow the natural time course of the ventricular action potential (through the voltage clamp), upon being simultaneously allowed to contribute current for the generation of this action potential as if they were incorporated into the membrane of the myocyte (through injection of the HERG current into the current-clamped myocyte).

The experiment of Fig. 6 directly demonstrates that the long-QT syndrome associated R56Q mutation results in significant action potential prolongation (Fig. 6B) and provides insights in the underlying mechanism (Fig. 6C). Notably, this action potential prolongation occurs

despite the larger initial HERG current in the mutant case. This demonstrates that the change in action potential profile is not only the result of changes in HERG current but also of changes in other membrane currents through their dependence on membrane potential.

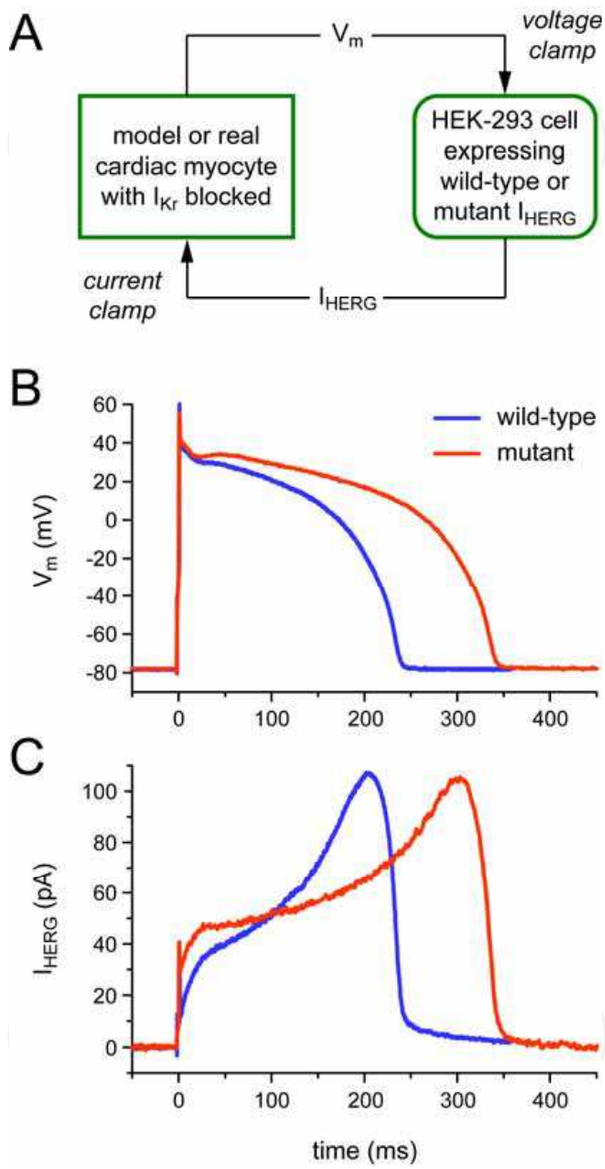

Fig. 6. Dynamic action potential clamp experiment, exploring the effect of the R56Q mutation in HERG. A single isolated rabbit ventricular myocyte was successively coupled to a HEK-293 cell expressing wild-type HERG current ('wild-type', blue traces) and a HEK-293 cell expressing R56Q mutant HERG current ('mutant', red traces). The myocyte had its native rapid delayed rectifier current (I_{Kr}) blocked by E-4031 and was paced at 1 Hz. (A) Experimental configuration. (B) Superimposed action potentials of the myocyte. (C) Associated HERG current. Data from Berecki et al. (2005).

The latter changes can be assessed using the recorded action potentials as voltage waveforms in traditional action potential clamp experiments or computer simulations. In the experiment of Fig. 6, WT and mutant HERG current were both scaled down to produce a HERG current density comparable to the native I_{Kr} density of the real isolated myocyte, as estimated using the I_{Kr} blocker E-4031. This scaling procedure seemed appropriate because the R56Q mutation is associated with altered gating properties rather than impaired trafficking of the HERG channel protein from the endoplasmic reticulum to the cell membrane.

5.3 Technical considerations

The experimental setup for the experiment of Fig. 6 is detailed in Fig. 7. The central desktop PC running the Real-Time Linux (RT-Linux) operating system (Barabanov & Yodaiken, 1997) is connected to two patch-clamp amplifiers, one in current clamp mode (amplifier 1) and the other in voltage clamp mode (amplifier 2). Through the command potential $V_{cmd,2}$ the central PC tells amplifier 2 to make the HEK-293 cell follow the free-running membrane potential of the myocyte. At the same time, through the command potential $V_{cmd,1}$, it tells amplifier 1 to inject the HERG current recorded from the HEK-293 cell into the myocyte. This is typically done with an update rate of 20 kHz, i.e. with the time step Δt set to 50 μs. Given the relatively high expression level of HERG channels in HEK-293 cells, the HERG current is scaled down to achieve an appropriate current amplitude. Any endogenous current included in the current recorded from the HEK-293 cell (Yu & Kerchner, 1998; Jiang et al., 2002) is then also scaled down, so that this endogenous current becomes negligible. However, if the expressed current needs to be scaled up, precautions should be made to avoid distortion by endogenous current, e.g. through a subtraction procedure as used in the study on sodium current by Berecki et al. (2006). The real isolated cardiac myocyte may be replaced by a real-time simulation of such cell, computed in the central PC. The differential equations of the mathematical model of the myocyte are then integrated with the above time step Δt.

As long as real-time simulations are not required, dAPC experiments can also be carried out using analogue circuitry, but if ease of use and high flexibility are important, the use of custom software running on an RT-Linux PC, or another operating system suitable for time-critical applications, equipped with a multifunction data acquisition board is the best option. Dynamic clamp software is not commercially available, but several research groups have made their custom software, mainly developed for use in neurophysiology, publicly available (Wilders, 2006). Our 'DynaClamp' dAPC software is available for download from our institutional website (URL: http://www.amc.nl/index.cfm?pid=4922).

As illustrated in Fig. 7, dAPC software should be able to continuously sample two analogue signals, carry out computations based on the acquired data, and send out two analogue signals based on the outcome of these computations. This implies that, in contrast with traditional data acquisition software, data buffering is not useful because individual samples are processed immediately after they are acquired. With today's computer processor speed the limiting factor for the overall speed (update rate) of the dAPC system is the rate of signal input and output operations, even if complex mathematical models are used in the computations of the current to be injected. With proper selection of hardware and software, an update rate of 10–50 kHz, corresponding with a cycle time of 20–100 μs, can be achieved. Considerations on this matter have been published elsewhere (see Wilders

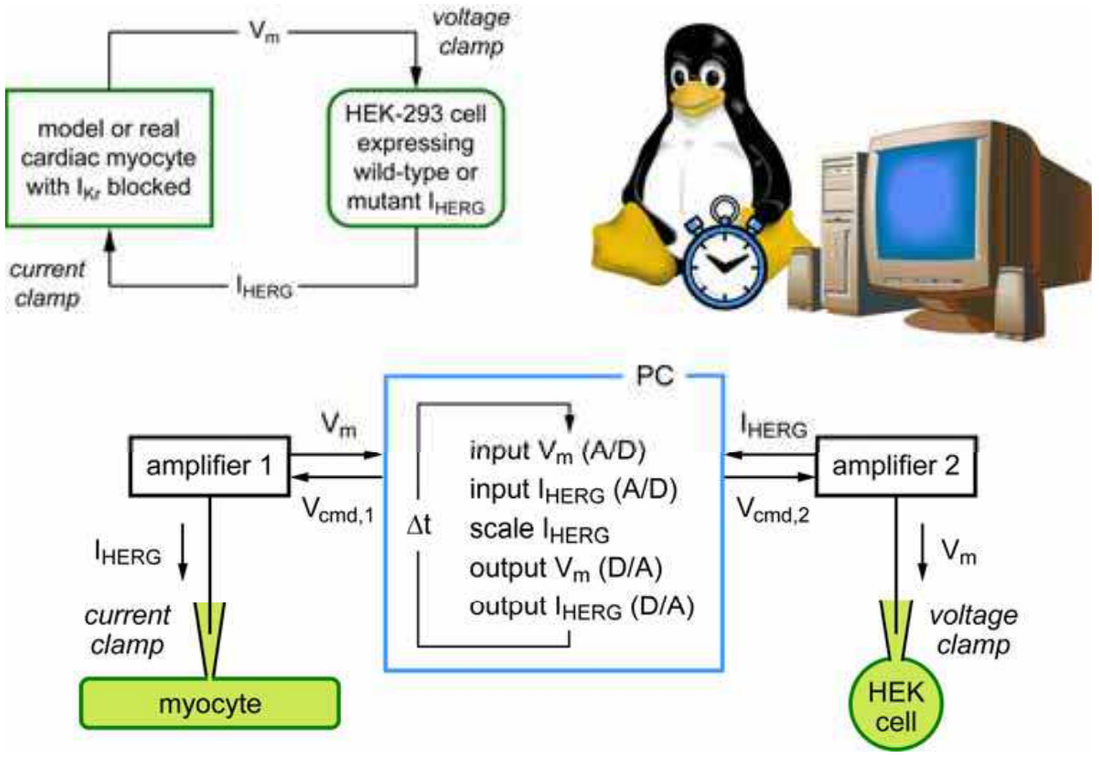

Fig. 7. Dynamic action potential clamp (dAPC) technique, when used to effectively replace the native HERG-encoded cardiac delayed rectifier potassium current (I_{Kr}) of a ventricular cell (or cell model) with the HERG current (I_{HERG}) recorded from a HEK-293 cell transfected with wild-type or mutant HERG cDNA. In a continuous cycle (with cycle time Δt), controlled through a PC running the Real-Time Linux (RT-Linux) operating system, I_{HERG} is recorded from the voltage-clamped HEK-293 cell, appropriately scaled, and then applied as external current to the ventricular myocyte, which is in current clamp mode and has its native I_{Kr} blocked pharmacologically (or set to zero in case of a model cell). The free-running action potential of the myocyte, co-shaped by the input I_{HERG}, is applied as voltage clamp command potential to the HEK-293 cell, thus establishing dAPC.

(2006) and primary references cited therein). In general, one should realize that carrying out dAPC experiments is not straightforward and that there are numerous distorting factors that should be taken care of (Bettencourt et al., 2008; Preyer & Butera, 2009).

6. Action potential clamp recordings of HCN4 current

With the availability of HEK-293 cells expressing HCN4 channels (Fig. 4), it is possible to record the HCN4 current that would flow during a prerecorded SA nodal action potential. We have carried out such traditional action potential clamp experiment, with the same electrophysiological recording conditions as for Fig. 4. We used the Wilders et al. (1991) rabbit SA nodal cell model with I_f set to zero to generate an action potential waveform and,

in a 10-s run, continuously applied the resulting action potential waveform to the HEK-293 cell as voltage clamp command potential (Fig. 8A; cf. Fig. 1A, red trace). Figure 8B shows the associated HCN4 current recorded from the HEK-293 cell.

There are several differences between the recorded HCN4 current (Fig. 8B) and the I_f 'pacemaker current' of the SA nodal cell model (Fig. 1C), which is computed from the second-order Hodgkin & Huxley type kinetic scheme put forward by van Ginneken & Giles (1991), based on their voltage clamp data on I_f obtained from rabbit SA nodal cells. Most strikingly, the HCN4 current has a large outward component, partly due to the more negative reversal potential of the HCN4 current (−43 mV in this particular cell, compared to −24 mV for the model I_f), and is available early during diastolic depolarization. Interestingly, the more pronounced outward component and early availability during

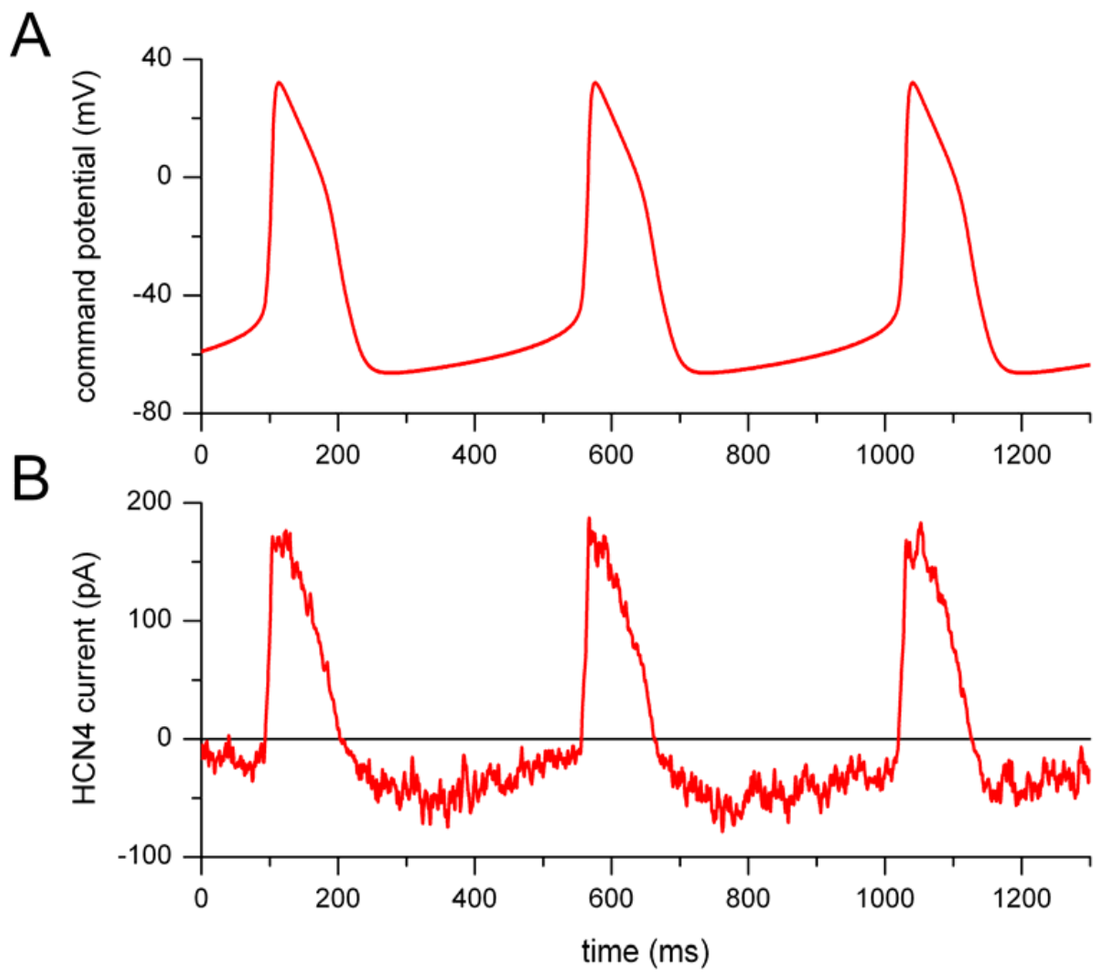

Fig. 8. Traditional action potential clamp experiment with a HEK-293 cell expressing HCN4 channels. (A) Sinoatrial (SA) nodal action potential waveform (Wilders et al. (1991) SA nodal cell model with I_f set to zero, cf. Fig. 1A) applied to the HEK-293 cell as voltage clamp command potential. (B) HCN4 current recorded from the HEK-293 cell.

diastole are in agreement with action potential clamp data from rabbit SA nodal cells by Zaza et al. (1997), who studied I_f as the current sensitive to 2 mmol/L Cs^+, and our recent numerical reconstructions, based on a first-order Hodgkin & Huxley type kinetic scheme, of I_f in human SA nodal cells (Verkerk et al., 2008; Verkerk et al., 2009a). The experiment of Fig. 8 underscores the importance of carrying out action potential clamp experiments in addition to traditional voltage clamp experiments and computer simulations.

7. Dynamic action potential clamp experiments with HCN4 current

The action potential clamp experiment of Fig. 8 reveals the HCN4 current that would flow during the prerecorded SA nodal action potential of Fig. 8A. However, it does not show how this current modulates the SA nodal action potential. Therefore, we also carried out a dynamic action potential clamp experiment with an HCN4-transfected HEK-293 cell in combination with the Wilders et al. (1991) model of a rabbit SA nodal pacemaker cell with its native I_f set to zero, as illustrated here in Fig. 9 and published elsewhere in the light of engineering a gene-based biological pacemaker (Verkerk et al., 2008; Verkerk et al., 2009c). A time step of 50 μs was used in the dAPC setup (cf. Fig. 7) and in the Euler type integration scheme that we used to solve the differential equations of the cell model.

In the Wilders et al. (1991) model, as in other (rabbit) SA nodal cell models (Wilders, 2007), the cycle length increases significantly upon blockade of I_f, mainly due to a decrease in the rate of diastolic depolarization (Fig. 1). As diagrammed in Fig. 9A, we used the action potential of the model cell—with its I_f set to zero—to voltage-clamp the HEK-293 cell and fed the recorded HCN4 current back into the current-clamped model cell, thus establishing the dAPC configuration. Given the large HCN4 currents expressed in HEK-293 cells (Fig. 4), we applied scaling factors of 0.0–1.0% to the recorded HCN4 current before adding it to the model. With the scaling factor set to zero (Fig. 9B, red trace labeled '0.0'), the resulting action potential is identical to that of the model cell with its I_f set to zero (Fig. 1A, red trace). With a scaling factor of 1.0% (Fig. 9B, blue trace labeled '1.0'), the cycle length shortens and becomes almost identical to that of the original model with its default I_f (Fig. 1A, blue trace). Intermediate shortening occurs with intermediate values for the scaling factor (Fig. 9B, traces labeled '0.5', '0.7' and '0.9').

The data of Fig. 9 suggest that the HCN4 current can functionally, in terms of modulating pacemaker frequency, replace the native I_f. However, unlike I_f, increasing the HCN4 current not only increases the rate of diastolic depolarization, but also clearly depolarizes the maximum diastolic potential to less negative values. This emphasizes that the kinetics of HCN4 channels need not be identical to those of native I_f channels (Qu et al., 2002) and that HCN4 channels should not simply be regarded as a replacement of I_f 'pacemaker channels' in gene therapy strategies. In addition, it stresses that the behaviour of HCN4 channels is more complex than reflected in the description of I_f in currently available SA nodal cell models (Wilders, 2007). A caveat that should be put in place here is that the depolarization of the maximum diastolic potential may, at least to some extent, be due to inward 'leakage current' of the HEK-293 cell, although the scaling factor of 0.01 or less also applies to this current. Ideally, the experiment of Fig. 9, and also that of Fig. 8, should have been carried with a human SA nodal cell model instead a rabbit model, but such model is not available due to a paucity of data from human SA nodal cells (Verkerk et al., 2007; Verkerk et al., 2009a; Verkerk et al., 2009b).

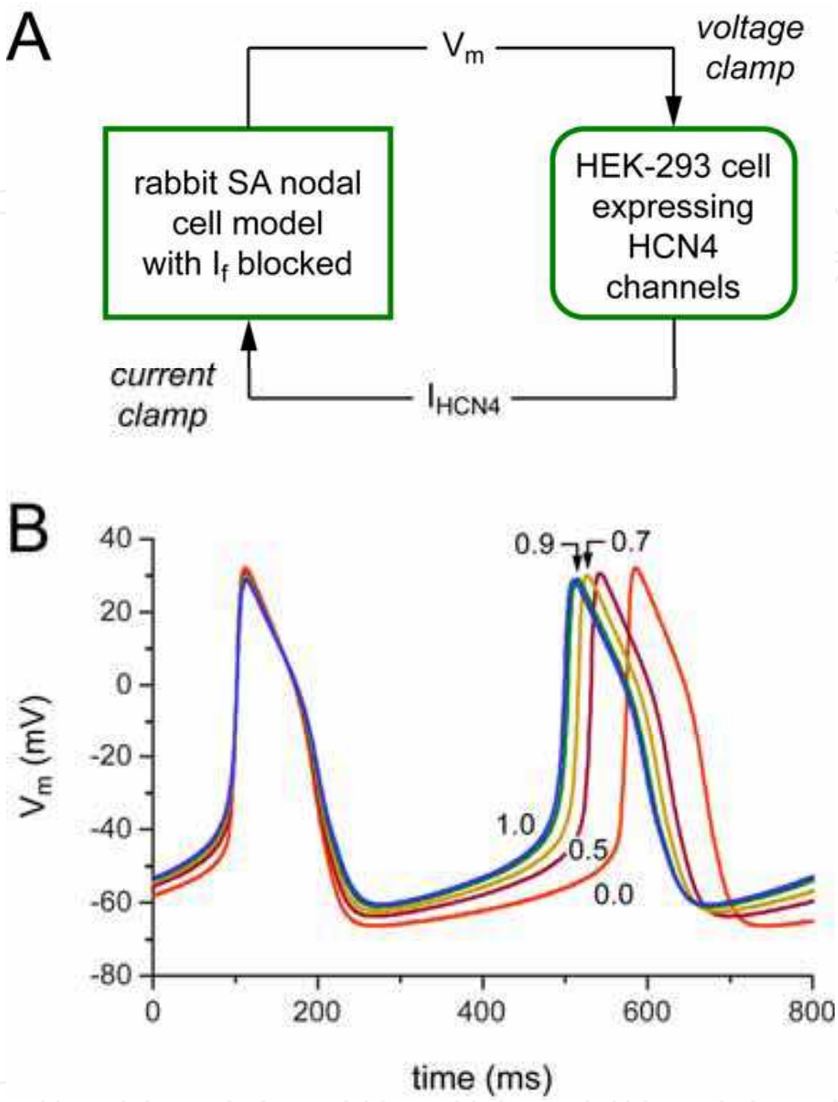

Fig. 9. Dynamic action potential clamp (dAPC) experiment with a real-time simulation of a sinoatrial (SA) nodal pacemaker cell and a HEK-293 cell expressing HCN4 channels. (A) Experimental configuration. An SA nodal pacemaker cell is simulated in real time using the Wilders et al. (1991) model of a rabbit SA nodal myocyte. The HCN-encoded hyperpolarization-activated current I_f, also known as 'pacemaker current' or 'funny current', of the model cell is set to zero and replaced with HCN4 current recorded from the HEK-293 cell (I_{HCN4}). (B) Effect of adding increasing amounts of HCN4 current to the SA nodal cell with its native I_f set to zero. A scaling factor of 0.0, 0.5, 0.7, 0.9, or 1.0%, as indicated by numbers near traces, was applied to the HCN4 current recorded from the HEK-293 cell.

8. Conclusion

In this chapter we have shown how our dynamic action potential clamp technique can provide important insights into the ionic mechanisms underlying intrinsic pacemaker activity of SA nodal cells. This underscores the important role that biomedical engineering can play in the field of cardiac cellular electrophysiology.

9. References

Barabanov, M. & Yodaiken, V. (1997). Introducing real-time Linux. *Linux Journal,* 34, February 1997, 19–23, ISSN: 1075-3583

Bellocq, C.; Wilders, R.; Schott, J.-J.; Louérat-Oriou, B.; Boisseau, P.; Le Marec, H.; Escande, D. & Baró, I. (2004). A common antitussive drug, clobutinol, precipitates the long QT syndrome 2. *Molecular Pharmacology,* 66, 5, 1093–1102, ISSN: 0026-895X

Berecki, G.; Zegers, J.G.; Verkerk, A.O.; Bhuiyan, Z.A.; de Jonge, B.; Veldkamp, M.W.; Wilders, R. & van Ginneken, A.C.G. (2005). HERG channel (dys) function revealed by dynamic action potential clamp technique. *Biophysical Journal,* 88, 1, 566–578, ISSN: 0006-3495

Berecki, G. & van Ginneken, A.C.G. (2006). Cardiac channelopathies studied with the dynamic action potential clamp technique. *Physiology News,* 63, Summer 2006, 28–29, ISSN: 1476-7996

Berecki, G.; Zegers, J.G.; Bhuiyan, Z.A.; Verkerk, A.O.; Wilders, R. & van Ginneken, A.C.G. (2006). Long-QT syndrome-related sodium channel mutations probed by the dynamic action potential clamp technique. *The Journal of Physiology,* 570, Pt. 2, 237–250, ISSN: 0022-3751

Berecki, G.; Zegers, J.G.; Wilders, R. & van Ginneken, A.C.G. (2007). Cardiac channelopathies studied with the dynamic action potential-clamp technique, In: *Patch-Clamp Methods and Protocols,* Molnar, P. & Hickman, J.J. (Eds.), 233–250, Humana Press, ISBN: 978-1-58829-698-6, Totowa, NJ, USA

Bettencourt, J.C.; Lillis, K.P.; Stupin, L.R. & White, J.A. (2008). Effects of imperfect dynamic clamp: computational and experimental results. *Journal of Neuroscience Methods,* 169, 2, 282–289, ISSN: 0165-0270

Boyett, M.R.; Honjo, H. & Kodama I. (2000). The sinoatrial node, a heterogeneous pacemaker structure. *Cardiovascular Research,* 47, 4, 658–687, ISSN: 0008-6363

Dobrzynski, H.; Boyett, M.R. & Anderson, R.H. (2007). New insights into pacemaker activity: promoting understanding of sick sinus syndrome. *Circulation,* 115, 14, 1921–1932, ISSN: 0009-7322

Goaillard, J.-M. & Marder, E. (2006). Dynamic clamp analyses of cardiac, endocrine, and neural function. *Physiology,* 21, 3, 197–207, ISSN: 1548-9213

Jiang, B.; Sun, X.; Cao, K. & Wang, R. (2002). Endogenous K_V channels in human embryonic kidney (HEK-293) cells. *Molecular and Cellular Biochemistry,* 238, 1-2, 69–79, ISSN: 0300-8177

Mangoni, M.E. & Nargeot, J. (2008). Genesis and regulation of the heart automaticity. *Physiological Reviews,* 88, 3, 919–982, ISSN: 0031-9333

Moosmang, S.; Stieber, J.; Zong, X.; Biel, M.; Hofmann, F. & Ludwig, A. (2001). Cellular expression and functional characterization of four hyperpolarization-activated

pacemaker channels in cardiac and neuronal tissues. *European Journal of Biochemistry,* 268, 6, 1646–1652, ISSN: 0014-2956

Preyer, A.J. & Butera, R.J. (2009). Causes of transient instabilities in the dynamic clamp. *IEEE Transactions on Neural Systems and Rehabilitation Engineering,* 17, 2, 190–198, ISSN: 1534-4320

Qu, J.; Altomare, C.; Bucchi, A.; DiFrancesco, D. & Robinson, R.B. (2002). Functional comparison of HCN isoforms expressed in ventricular and HEK 293 cells. *Pflügers Archiv - European Journal of Physiology,* 444, 5, 597–601, ISSN: 0031-6768

Qu, J.; Kryukova, Y.; Potapova, I.A.; Doronin, S.V.; Larsen, M.; Krishnamurthy, G.; Cohen, I.S. & Robinson, R.B. (2004). MiRP1 modulates HCN2 channel expression and gating in cardiac myocytes. *The Journal of Biological Chemistry,* 279, 42, 43497–43502, ISSN: 0021-9258

van Ginneken, A.C.G. & Giles, W. (1991). Voltage clamp measurements of the hyperpolarization-activated inward current I_f in single cells from rabbit sino-atrial node. *The Journal of Physiology,* 434, Pt. 1, 57–83, ISSN: 0022-3751

Varghese, A.; TenBroek, E.M.; Coles, J. Jr. & Sigg, D.C. (2006). Endogenous channels in HEK cells and potential roles in HCN ionic current measurements. *Progress in Biophysics and Molecular Biology,* 90, 1–3, 26–37, ISSN: : 0079-6107

Verkerk, A.O.; Wilders, R.; van Borren, M.M.G.J.; Peters, R.J.G.; Broekhuis, E.; Lam, K.Y.; Coronel, R.; de Bakker, J.M.T. & Tan, H.L. (2007). Pacemaker current (I_f) in the human sinoatrial node. *European Heart Journal*, 28, 20, 2472–2478, ISSN: 0195-688X

Verkerk, A.O., Zegers, J.G., van Ginneken, A.C.G. & Wilders, R. (2008). Dynamic action potential clamp as a powerful tool in the development of a gene-based bio-pacemaker. *Conference Proceedings of the IEEE Engineering in Medicine and Biology Society,* 2008, 1, 133–136, ISSN: 1557-170X

Verkerk, A.O., van Ginneken, A.C.G. & Wilders, R. (2009a). Pacemaker activity of the human sinoatrial node: role of the hyperpolarization-activated current, I_f. *International Journal of Cardiology,* 132, 3, 318–336, ISSN: 0167-5273

Verkerk, A.O.; Wilders, R.; van Borren, M.M.G.J. & Tan, H.L. (2009b). Is sodium current present in human sinoatrial node cells? *International Journal of Biological Sciences,* 5, 2, 201–204, ISSN: 1449-2288

Verkerk, A.O., Zegers, J.G., van Ginneken, A.C.G. & Wilders, R. (2009c). Development of a genetically engineered cardiac pacemaker: insights from dynamic action potential clamp experiments, In: *Dynamic-Clamp: From Principles to Applications,* Destexhe, A. & Bal, T. (Eds.), 399–415, Springer, ISBN: 978-0-387-89278-8, New York, NY, USA

Wilders, R.; Jongsma, H.J. & van Ginneken, A.C.G. (1991). Pacemaker activity of the rabbit sinoatrial node: a comparison of mathematical models. *Biophysical Journal,* 60, 5, 1202–1216, ISSN: 0006-3495

Wilders, R. (2005). 'Dynamic clamp' in cardiac electrophysiology. *The Journal of Physiology,* 566, Pt. 2, 641, ISSN: 0022-3751

Wilders, R. (2006). Dynamic clamp: a powerful tool in cardiac electrophysiology. *The Journal of Physiology,* 576, Pt. 2, 349–359, ISSN: 0022-3751

Wilders, R. (2007). Computer modelling of the sinoatrial node. *Medical & Biological Engineering & Computing,* 45, 2, 189–207, ISSN: 0140-0118

Yu, S.P. & Kerchner, G.A. (1998). Endogenous voltage-gated potassium channels in human embryonic kidney (HEK293) cells. *Journal of Neuroscience Research,* 52, 5, 612–617, ISSN: 0360-4012

Zaza, A.; Micheletti, M.; Brioschi, A. & Rocchetti, M. (1997). Ionic currents during sustained pacemaker activity in rabbit sino-atrial myocytes. *The Journal of Physiology,* 505, Pt. 3, 677–688, ISSN: 0022-3751

Biomedical Engineering

Edited by Carlos Alexandre Barros de Mello

ISBN 978-953-307-013-1
Hard cover, 658 pages
Publisher InTech
Published online 01, October, 2009
Published in print edition October, 2009

Biomedical Engineering can be seen as a mix of Medicine, Engineering and Science. In fact, this is a natural connection, as the most complicated engineering masterpiece is the human body. And it is exactly to help our "body machine" that Biomedical Engineering has its niche. This book brings the state-of-the-art of some of the most important current research related to Biomedical Engineering. I am very honored to be editing such a valuable book, which has contributions of a selected group of researchers describing the best of their work. Through its 36 chapters, the reader will have access to works related to ECG, image processing, sensors, artificial intelligence, and several other exciting fields.

INTECH
open science | open minds

InTech Europe
University Campus STeP Ri
Slavka Krautzeka 83/A
51000 Rijeka, Croatia
Phone: +385 (51) 770 447
Fax: +385 (51) 686 166
www.intechopen.com

InTech China
Unit 405, Office Block, Hotel Equatorial Shanghai
No.65, Yan An Road (West), Shanghai, 200040, China
中国上海市延安西路65号上海国际贵都大饭店办公楼405单元
Phone: +86-21-62489820
Fax: +86-21-62489821

IntechOpen